The microscopic pairing gap in a slab of nuclear matter for the Argonne v_{18} NN-potential

S. S. Pankratov[a], M. Baldo[b], U. Lombardo[c,d], E.E. Saperstein[a] and M .V. Zverev[a]

[a] Kurchatov Institute, 123182, Moscow, Russia
[b]INFN, Sezione di Catania, 64 Via S.-Sofia, I-95123 Catania, Italy
[c]INFN-LNS, 44 Via S.-Sofia, I-95123 Catania, Italy
[d] 44 Via S.-Sofia, I-95123 Catania, Italy

Abstract

Ab initio gap equation for $^1S_0$ pairing in a nuclear slab is solved for the Argonne v_{18} NN-potential. The gap function is compared in detail with the one found previously for the separable form of the Paris potential. The difference between the two gaps turned out to be about 10%. Dependence of the gap on the chemical potential μ is analyzed.

1 Introduction

In the last decade, a progress was reached in the microscopic theory of pairing in atomic nuclei. In this connection, the studies of the Milan group [1, 2] should be cited first. In the recent paper [2] the direct solution of the *ab initio* gap equation for a nucleus ^{120}Sn was carried out using the realistic Argonne v_{14} NN-potential. A bit later we made a similar calculation [3] for a slab of nuclear matter with parameters mimicking the atomic nuclei of the tin region with the Paris potential [4]. The comparison of results of these two calculations rises some questions. In Ref. [2] the gap Δ, obtained by solving the gap equation, turned out to be about a half of the experimental value. The discrepancy was attributed to the missing contribution of the low-lying surface vibrations[2]. On the other hand, the gap found in [3] is much closer to the experimental one and leaves a room to the surface vibration corrections only for a 20% about.

To some extent, the difference could originate from the difference between the two systems under consideration, the spherical nucleus and the slab. This reason seems to us not very important as far as only the curvature effects make the difference. Different values of the effective nucleon mass m^* used in these two alternative calculations look more essential. Indeed, it is well known [5] that the gap value in infinite matter is rather sensitive to the value of the effective mass m^*. In [2] the coordinate dependent effective mass $m^*(r)$ was used of the Sly4 version [6] of the Skyrme force. Its value changes from $m^* = 0.7m$ inside a nucleus to $m^* = m$ outside. In [3] the bare nucleon mass, $m^* = m$, was used, in accordance with prescriptions of [7] and [8]. The specific form of the realistic NN-potential used in the gap equation is one more possible reason of the difference under discussion. In this article we analyze the latter point repeating the calculation of [3], but for the Argonne v_{18} potential [9] which is quite similar to that of [2] but essentially different from the Paris potential. Indeed, both the version of the Argonne force are rather soft core whereas the Paris potential is one of the most hard core realistic NN-potentials. In addition, we examine the dependence of the pairing gap on the chemical potential μ of the system under consideration.

2 The formalism

The general method for solving the gap equation in a system with the 1D inhomogeneity is developed in Ref. [3]. Here we present only the formalism which is necessary to describe the procedure. Just as in Ref [3], we use the two-step method [10] to solve the microscopic gap equation,

$$\Delta = \mathcal{V} A^s \Delta, \tag{1}$$

where $\mathcal{V}$ is the free NN-potential and $A^s = GG^s$ stands for the two-particle propagator in the superfluid system. Here G and G^s are the one-particle Green functions without and with pairing effects taken into account, respectively. In Eq. (1), as usual, integration over intermediate coordinates and summation over spin variables is understood. In the nuclear matter theory, the gap equation in the form of Eq. (1) is usually referred to as the Bardeen–Cooper–Schrieffer (BCS) approximation.[1] In the more profound many-body theory [11, 12] the irreducible block of the NN-interaction should replace $\mathcal{V}$ in Eq. (1).

The complete Hilbert space S of two-particle states is split into two parts, $S = S_0 + S'$. The first one is the model subspace S_0 in which the gap equation is considered, and the other is the complementary subspace S'. They are separated by the energy E_0 in such a way that S_0 involves all the two-particle states (λ, λ') with the single-particle energies $\varepsilon_\lambda, \varepsilon_{\lambda'} < E_0$. The complementary subspace S' involves such two-particle states for which one of the energies $\varepsilon_\lambda, \varepsilon_{\lambda'}$ or both of them are greater than E_0. Therefore, pairing effects can be neglected in S' if E_0 is sufficiently large. Validity of the inequality $\Delta^2/(E_0 - \mu)^2 \ll 1$ is the criterium of such approximation.

Correspondingly, the two-particle propagator is represented as the sum $A^s = A^s_0 + A'$. Here we already neglected the superfluid effects in the S'-subspace and omitted the superscript "s" in the second term. The gap equation (1) can be rewritten in the model subspace,

$$\Delta = V^p_{\text{eff}}\, A^s_0\, \Delta\,, \tag{2}$$

where the effective pairing interaction (EPI) should be found in the supplementary subspace,

$$V^p_{\text{eff}} = \mathcal{V} + \mathcal{V} A'\, V^p_{\text{eff}}\,. \tag{3}$$

[1] In physics of finite nuclei this term is commonly used for an approximate way to solve the pairing problem, contrary to solving the Bogolyubov equations.

As is well known, the gap equation (1) can be written in an equivalent form,

$$\Delta = -\mathcal{V}\varkappa, \tag{4}$$

where the anomalous density matrix $\varkappa$ is expressed directly in terms of the Bogolyubov u-, v-functions:

$$\varkappa(\mathbf{r}_1, \mathbf{r}_2) = \sum_i u_i(\mathbf{r}_1) v_i(\mathbf{r}_2). \tag{5}$$

The summation in (5) is carried out over the complete set of the Bogolyubov functions with eigenenergies $E_i > 0$.

The gap equation (2) in the model subspace can be also written in a form similar to (4),

$$\Delta = -V^p_{\rm eff}\varkappa_0\,, \tag{6}$$

where $\varkappa_0$ is the anomalous density matrix specified in the model subspace as

$$\varkappa_0(\mathbf{r}_1, \mathbf{r}_2) = \int A^s_0(E; \mathbf{r}_1, \mathbf{r}_2, \mathbf{r}_3, \mathbf{r}_4)\Delta(\mathbf{r}_3, \mathbf{r}_4) d\mathbf{r}_3 d\mathbf{r}_4\,. \tag{7}$$

However, a simple expression for this quantity similar to Eq. (5) does not exist. To obtain the explicit form of $\varkappa_0$ it is convenient to use the basis of the single-particle functions $\phi_\lambda(\mathbf{r})$ which makes the normal Green function G diagonal: $G_{\lambda\lambda'}(\varepsilon)$=$G_\lambda(\varepsilon)\delta_{\lambda\lambda'}$. Then one gets:

$$u_i(\mathbf{r}) = \sum_\lambda u_i^\lambda \phi_\lambda(\mathbf{r}), \tag{8}$$

$$v_i(\mathbf{r}) = \sum_\lambda v_i^\lambda \phi_\lambda(\mathbf{r}), \tag{9}$$

$$\Delta(\mathbf{r}_1, \mathbf{r}_2) = \sum_{\lambda,\lambda'} \Delta_{\lambda\lambda'}\phi_\lambda(\mathbf{r}_1)\phi_{\lambda'}(\mathbf{r}_2). \tag{10}$$

After a simple algebra [3], one finds

$$\varkappa_0(\mathbf{r}_1, \mathbf{r}_2) = \sum_{i,\lambda_1,\lambda_2}^{(0)} \left(n_{\lambda_1}\, u_i^{\lambda_1}\, v_i^{\lambda_2} + (1 - n_{\lambda_1})\, u_i^{\lambda_2}\, v_i^{\lambda_1}\right) \phi_{\lambda_1}(\mathbf{r}_1)\phi_{\lambda_2}(\mathbf{r}_2), \tag{11}$$

where $n_\lambda = (0; 1)$ are the occupation numbers without pairing. The superscript "(0)" in the sum means that all the states λ belong to the model

subspace: $\varepsilon_\lambda < E_0$. It can be easily seen that in the limit of $E_0 \to \infty$, when the set $\{\lambda\}$ is complete, the expression (11) coincides with Eq. (5).

We consider a slab of nuclear matter embedded into the one-dimensional potential $U(x)$. In this case, the momentum $\mathbf{k}_\perp$ in the (y,z)-plane (or $\mathbf{s}$-plane) is an integral of motion. The single-particle wave functions can be written as

$$\phi_\lambda(\mathbf{r}) = e^{i\mathbf{k}_\perp \mathbf{s}} y_n(x), \tag{12}$$

and the Bogolyubov functions have the form:

$$u_i(\mathbf{r}) = e^{i\mathbf{k}_\perp \mathbf{s}}\, u_i(k_\perp, x) \tag{13}$$

$$v_i(\mathbf{r}) = e^{i\mathbf{k}_\perp \mathbf{s}}\, v_i(k_\perp, x)\,, \tag{14}$$

Just as in Ref. [3], we will use the mixed representation, i.e., the coordinate representation for the x-direction and the momentum one for the $\mathbf{s}$-plane. The scheme of solving the gap equation in the mixed representation was developed in detail in [3] for the case of the separable form of the Paris potential [13, 14]. Now we consider the original form of the Argonne v_{18} potential [9] and present the main formulas for the general case.

Let us begin with the EPI. In the Wigner representation it depends on the relative momenta $\mathbf{k}_1$ and $\mathbf{k}_2$ and on the CM coordinates X_1 and X_2 in the input and the output channel. As far as we deal with the singlet pairing, the zeroth harmonic of the EPI enters into the gap equation which depends only on the absolute value of the relative momenta. One more advantage of the two-step method is the possibility of using the so-called local potential approximation (LPA) [10] to find the EPI. According to the LPA, the EPI at each point $X = (X_1 + X_2)/2$ can be replaced by the one in infinite nuclear matter placed in the external potential field $U(X)$:

$$V_{\mathrm{eff}}^{\mathrm{LPA}}(k_1, k_2; X_1, X_2) = V_{\mathrm{eff}}^{\mathrm{inf}}(k_1, k_2; t, [U(X)]), \tag{15}$$

where $t{=}X_1 - X_2$. To find the EPI in infinite system, it is convenient first to solve the Lippman-Schwinger equation in the complementary subspace in momentum space,

$$V_{\mathrm{eff}}^{\mathrm{inf}}(k_1, k_2, P; E) = \mathcal{V}(k_1, k_2) + \int_{\mathbf{k}\in S'} \frac{d^3k}{(2\pi)^3} \frac{\mathcal{V}(k_1, k) V_{\mathrm{eff}}^{\mathrm{inf}}(k, k_2, P; E)}{E - \varepsilon(\mathbf{P}, \mathbf{k}) - \varepsilon'(\mathbf{P}, \mathbf{k})}, \tag{16}$$

where $E = 2\mu$, $\varepsilon(\mathbf{P}, \mathbf{k}) = (\mathbf{P}/2 + \mathbf{k})^2/(2m) + U(X)$, $\varepsilon'(\mathbf{P}, \mathbf{k}) = (\mathbf{P}/2 - \mathbf{k})^2/(2m) + U(X)$. The integration in (16) is carried out over $\mathbf{k} \in S'$. The

quantity $V_{\rm eff}^{\rm inf}(k_1,k_2;t,[U(X)])$ is found from $V_{\rm eff}^{\rm inf}(k_1,k_2;P,[U(X)])$ with the inverse Fourier transformation.

The explicit form of the gap equation (6) in the Wigner representation for the 1D geometry is as follows:

$$\Delta(k,X) = -\int V_{\rm eff}^{p}(k,k';X,X')\,\varkappa_0(k'_{\perp},k'_x;X')\,\frac{d^2\mathbf{k}'_{\perp}}{(2\pi)^2}\,\frac{dk'_x}{2\pi}\,dX'\,, \qquad (17)$$

The anomalous density can be written as

$$\varkappa_0(k_{\perp},k_x;X) = \sum_{nn'}^{(0)} \varkappa_0^{nn'}(k_{\perp})\,f_{nn'}(k_x,X)\,, \qquad (18)$$

where

$$f_{nn'}(k_x,X) = \int e^{-i\,k_x\,x}\,y_n(X+x/2)\,y_{n'}(X-x/2)\,dx\,, \qquad (19)$$

and

$$\varkappa_0^{nn'}(k_{\perp}) = \sum_{i}^{(0)} \Big(n_{k_{\perp}n}\,u_i^n(k_{\perp})\,v_i^{n'}(k_{\perp}) + (1-n_{k_{\perp}n})\,u_i^{n'}(k_{\perp})\,v_i^n(k_{\perp}) \Big)\,. \qquad (20)$$

Here we used the expansion of the Bogolyubov functions into the basis $\{y_n\}$:

$$u_i(k_{\perp},x) = \sum_{n}^{(0)} u_i^n(k_{\perp})\,y_n(x)\,, \quad v_i(k_{\perp},x) = \sum_{n}^{(0)} v_i^n(k_{\perp})\,y_n(x)\,. \qquad (21)$$

In this representation, the Bogolyubov equations have the form:

$$\begin{cases} (\varepsilon_{nk_{\perp}}-\mu)\,u_i^n(k_{\perp}) + \sum\limits_{n'} \Delta_{nn'}(k_{\perp})\,v_i^{n'}(k_{\perp}) = E_i\,u_i^n(k_{\perp})\,, \\ \sum\limits_{n'} \Delta_{nn'}(k_{\perp})\,u_i^{n'}(k_{\perp}) - (\varepsilon_{nk_{\perp}}-\mu)\,v_i^n(k_{\perp}) = E_i\,v_i^n(k_{\perp})\,, \end{cases} \qquad (22)$$

where $\varepsilon_{nk_{\perp}}=\varepsilon_n + {k_{\perp}}^2/2m$ and

$$\begin{aligned} \Delta_{nn'}(k_{\perp}) &= \int \Delta(k_{\perp},x,X)\,y_n(X+\frac{x}{2})\,y_{n'}(X-\frac{x}{2})\,dx\,dX = \\ &= \int \Delta(k,X)\,f_{nn'}(k_x,X)\,dX\,\frac{dk_x}{2\pi}\,. \end{aligned} \qquad (23)$$

The chemical potential μ in (22) is determined inverting the equation for the number of particles per a unit surface of the slab:

$$\sigma = \int \frac{d^2\mathbf{k}_\perp}{(2\pi)^2} \sum_{i\lambda} \left(v_i^\lambda(k_\perp)\right)^2 = \text{const}\,. \tag{24}$$

The above relations determine the gap function in the slab system.

3 Calculation results

Just as in [3], we use the Saxon-Woods potential $U(x)$ symmetrical with respect to the point $x = 0$ with typical for finite nuclei values of the potential well depth $U_0 = -50$ MeV and diffuseness parameter of $d = 0.65$ fm. For the main part of calculations the thickness parameter of the slab was chosen as $L = 6$ fm to mimic nuclei of the tin region. As far as the Hamiltonian of the system is symmetrical under the axis reflection $x \to -x$, the eigenfunctions y_n can be separated into even, y_n^+, and odd, y_n^-, functions. It simplifies the numerical procedure essentially, as far the n, n' indices in (22) should numerate the states of a fixed parity.

The calculation scheme is rather different from that used in [3] for the separable form of the NN-force. The common feature is the convenience to use the scheme of parallel calculations for different $k_\perp$ momentum, since the slab is homogeneous in the $\mathbf{s}-$plane. The total number of processors we used is 210, which gives required accuracy for calculations with the model space S_0 specified by $E_0 = 15$ MeV. The discrete spectrum representation method was used to take into account the continuum, $0 < \varepsilon_\lambda < E_0$. The infinite wall was put at the distance $R = 25$ fm. The independence of results on the value of R was checked. The gap equation (17) was solved with iterations. The procedure was stopped when the maximal difference of values of $\Delta(k, X)$ obtained in two subsequent iterations became less than 10^{-6} MeV. The typical number of effective iterations was about 10. The chemical potential was found anew according (24) on each iteration. The self-consistent value of the chemical potential $\mu = -7.95$ MeV is very close to the one, $\mu_0 = -8$ MeV, without pairing. The difference $\delta\mu = -0.05$ MeV is in agreement with the standard estimate $\delta\mu \sim -\Delta^2/\varepsilon_\mathrm{F}$.

To illustrate the solution graphically, we calculated the "Fermi averaged" gap

$$\Delta_\mathrm{F}(X) = \Delta(k_\mathrm{F}(X), X). \tag{25}$$

Here the local Fermi momentum is defined as follows: $k_{\rm F}^2(X)$=$2m(\mu-U(X))$ if $2m(\mu-U(X)) > 0$, and $k_{\rm F}^2(X)$=0 otherwise. Analogously, we could define the Fermi averaged EPI as

$$\mathcal{V}_{\rm eff}^{\rm F}(X) = \int dt V_{\rm eff}^{p}(k_1{=}k_2{=}k_{\rm F}(X); t, X). \tag{26}$$

There are two parameters which influence essentially difficulties of the calculation procedure. They are the separation energy E_0 which defines the model space S_0 and the cut-off momentum $K_{\rm max}$ in the integral of Eq. (16). Let us begin from choosing the first one. Fig. 1 shows the dependence of the solution on the value of E_0. Analyzing these curves one can see that the variation of E_0 from 5 MeV to 10 MeV results in the change of the maximum of the Fermi-averaged gap function of the order of 5% whereas the next step to 15 MeV diminishes this difference to 1%. A more quantitative information could be obtained from the matrix elements of the gap. The diagonal matrix elements $\Delta_{nn}(k_\perp{=}0)$ for different E_0 are presented in Table 1. The even states are located in the upper part of the table, the odd ones, in the lower part. One can see that the convergence of Δ_{nn} values increasing E_0 is slower than that of the maximum of $\Delta_{\rm F}(X)$. Now the average change of a matrix element with the variation of E_0 from 10 MeV to 15 MeV is about 3%. This is, of course, the upper estimate of the accuracy if we choose $E_0 = 15$ MeV as an appropriate value. Analyzing the convergence of Δ_{nn} values in Table 1, one can suppose that the change under consideration will be about 1-2% at the next step to $E_0 = 20$ MeV. Therefore more realistic estimate of the accuracy of the calculations for $E_0 = 15$ MeV is 1-2%.

The latter could be referred to both approximations used in the version of the the two-step approach outlined in Sect. 2. These are: neglecting of the pairing in the complementary space S' and using the LPA as well. Note that in the case of the Paris potential 1% accuracy was reached at $E_0 = 20$ MeV [3].

Let us turn now to the analysis of dependence of the gap function on the cut-off momenta $K_{\rm max}$ in Eq. (16). The Fermi-averaged gap $\Delta_{\rm F}(X)$ is displayed in the left panel of Fig. 2 for different $K_{\rm max}$ in the case of the Argonne v_{18} potential. The value of $K_{\rm max} = 6.2$ fm^{-1} corresponds to the cut-off energy $E_{\rm max} = 800$ MeV used in [2]. We see that this value of $K_{\rm max}$ guarantees only 10% accuracy of the gap value and only $K_{\rm max} = 10$ fm^{-1} is sufficiently big to result in 1% accuracy. Therefore it is possible that the gap found in [2] is underestimated at approximately 10% due to not sufficiently

Table 1: Diagonal matrix elements $\Delta_{nn}(k_{\perp}=0)$ (MeV) in the slab with the width parameter L=6 fm for Argonne v_{18} potential for different E_0 (MeV). ε_n (MeV) is the single particle spectrum.

ε_n	Δ_{nn}			
	$E_0 = 0$	$E_0 = 5$	$E_0 = 10$	$E_0 = 15$
-48.26	1.516	1.362	1.339	1.284
-36.55	1.461	1.282	1.245	1.210
-18.60	1.198	1.034	0.982	0.972
-1.325	0.421	0.342	0.324	0.309
-43.51	1.522	1.339	1.309	1.266
-28.04	1.353	1.174	1.119	1.102
-9.10	0.903	0.764	0.747	0.717

big value of $E_{\max}$. Note that another version of the Argonne force, v_{14}, was used there but it is quite close to that used by us. In the systematic calculations, the values of $E_0 = 15$ MeV and $K_{\max} = 10$ fm^{-1} will be chosen.

For comparison, the analogous dependence is shown for the Paris potential in the right panel of Fig. 2 demonstrating very slow convergence of the integral in Eq. (16) in this case. Indeed, now the huge value of $K_{\max} = 160$ fm^{-1} is necessary to guarantee 1% accuracy for the Paris potential. Only the use of the separable version of the Paris force in [3] made it possible to carry out calculations with sufficient accuracy.

Fig. 3 demonstrates that the EPI found from Eq. (16) depends only a little on the specific form of the realistic NN-potential used provided the convergence of the integral in the momentum space is reached. One can see that the two curves for different potentials are nearly coincident. To show a small difference we displayed the same curves at small and large values of x separately in a large scale. We see that the difference is about 2% in the asymptotic region where the EPI is big and about 5% where the EPI is small. However, even such a small variation of the EPI is not negligible as far as any change of the pairing force is significantly enhanced in the gap equation. As the analysis of [3] has shown, in the system under consideration a 1% variation of the EPI results in approximately 5% variation of the gap. It is confirmed with direct comparison of the gap functions for both the

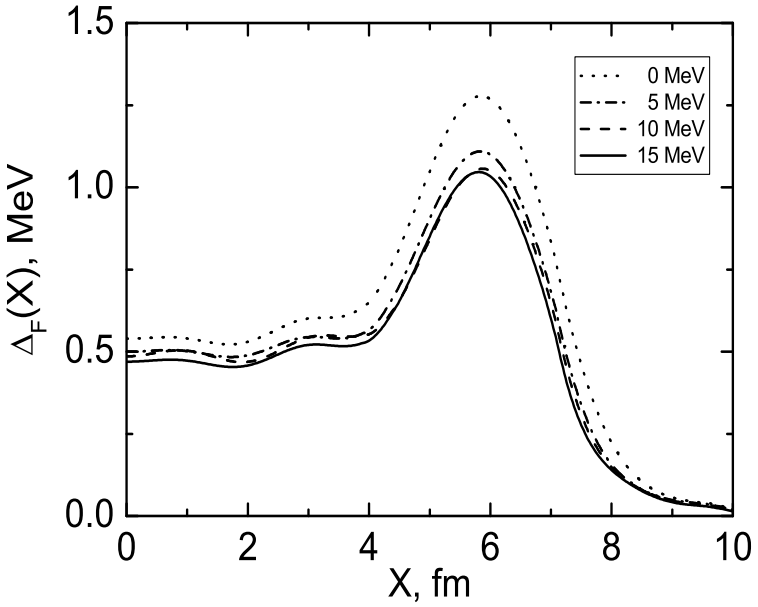

Figure 1: The Fermi averaged gap $\Delta_{\rm F}(X)$ for different E_0.

potentials which is presented in Fig. 4. The maximual difference between values of $\Delta_{\rm F}(X)$ for different potentials is of the order of 10%.

To analyze this difference quantitatively it is instructive to compare the matrix elements of the gap. They are presented in Table 2 for the diagonal matrix elements $\Delta_{nn}(k_\perp{=}0)$. One can see that the difference under consideration is again of the order of 10%. The only exception is the state with very small energy $\varepsilon_n{=}-1.3$ MeV for which the matrix element of Δ itself is essentially less than the typical values which is of the order of 1 MeV. This peculiarity of states with small energy is caused with a special form of their wave functions which have very long "tails" outside the slab. Therefore the weight of $y_n(x)^2$ in the integral of Δ_{nn} is rather small in the region where the $\Delta(X)$ is large. The upper half of the table contains the positive parity states. These are the matrix elements which could be related to those in heavy nuclei over the single-particle s-states. Indeed, the $k_\perp$ variable in a slab is an analogue of the orbital angular momentum l in a spherical nucleus, $k_\perp = 0$ corresponding to $l = 0$. The average value of $\Delta_{nn}(k_\perp{=}0)$ for the positive parity states is $\bar{\Delta}$=0.94 MeV for the Argonne force and =1.04 MeV for the Paris potential. It looks reasonable to exclude the state with anoma-

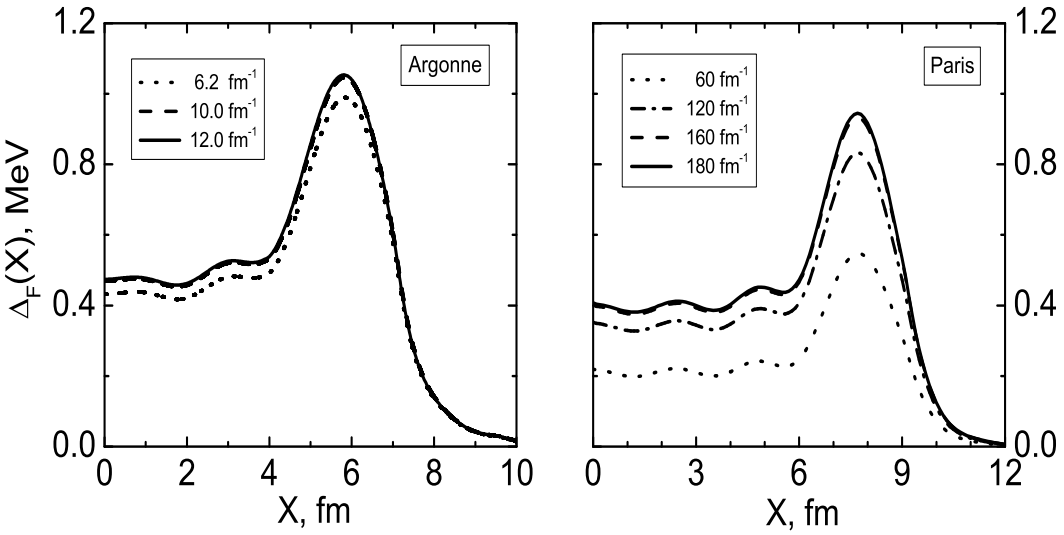

Figure 2: The Fermi averaged gap $\Delta_{\rm F}(X)$ for different cut-off momenta $K_{\rm max}$ (in fm^{-1}) for the Argonne v_{18} potential (the left panel, $E_0 = 15$ MeV) and the Paris potential (the right panel, $E_0 = 20$ MeV).

lously small energy for calculating the average value of the gap. In this case, one finds $\bar{\Delta}$=1.16 MeV for the Argonne force and =1.27 MeV for the Paris potential. These values should be compared with the experimental values of the gap in the tin region which are of the order of $\Delta_{\rm exp} \simeq 1.3$ MeV. We see that although the gap value for the Argonne force is a little (10%) less than that for the Paris force it is also rather close to the experimental data, reserving only narrow room ($\simeq 10 - 20\%$) for contributions of the surface vibrations.

The quantity $\Delta_{\rm F}(X)$ is a localized representation of the gap. To examine the nonlocal properties of the gap, it is reasonable to calculate the X-dependent rms radius

$$r_\Delta(X) = \sqrt{\langle r^2_\Delta(X)\rangle}\,, \tag{27}$$

where

$$\langle r^2_\Delta(X)\rangle = \frac{\int \mathbf{r}^2\Delta(r,X)\; d^3\mathbf{r}}{\int \Delta(r,X)\; d^3\mathbf{r}} = \left.\frac{-\dfrac{\partial^2}{\partial k^2}\Delta(k,X)}{\Delta(k,X)}\right|_{k=0}. \tag{28}$$

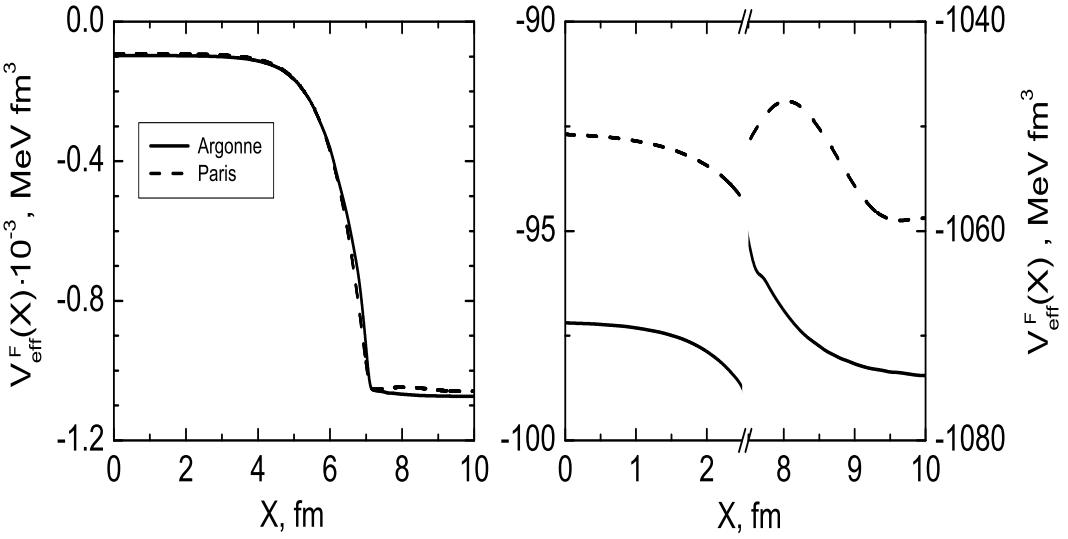

Figure 3: The Fermi averaged EPI $\mathcal{V}^{\rm F}_{\rm eff}(X)$ for the Argonne v_{18} potential (solid line) and the Paris potential (dashes), $E_0 = 20$ MeV) for both the cases.

It is displayed in Fig. 5. We see that it is about 0.8 fm inside the slab and grows to $\simeq 1.2$ fm outside, i.e. the gap function is essentially non-local.

4 On the μ-dependence of the gap

In this section, we analyze dependence of the pairing gap on the chemical potential μ. This subject is of interest due to a progress in physics of of nuclei laying far off the β-stability valley reached in recent years. In particular, it concerns nuclei in the vicinity of the nucleon drip line, where the chemical potential μ of the neutron or the proton subsystem vanishes. The importance of nucleon pairing for this region is generally accepted. In studies aimed at calculating the nucleon drip line within the Hartree–Fock method [15, 16] or the generalized EDF method [8], which employ a phenomenological nucleon–nucleon interaction, much attention was given to exploring special features of pairing at small values of μ. In this connection, the main interest was put to such problems as the correct taking into account continuum states, as a comparison of the exact solution of the Bogolyubov equations with that found within the BCS approximation, and so on. However, the possibility

Table 2: Diagonal matrix elements $\Delta_{nn}(k_{\perp}=0)$ (MeV) in the slab with the width parameter L=6 fm. ε_n (MeV) is the single particle spectrum.

ε_n	Δ_{nn}	
	Argonne v_{18} potential	Paris potential
-48.26	1.284	1.396
-36.55	1.210	1.326
-18.60	0.972	1.077
-1.325	0.309	0.357
-43.51	1.266	1.385
-28.04	1.119	1.227
-9.10	0.764	0.817

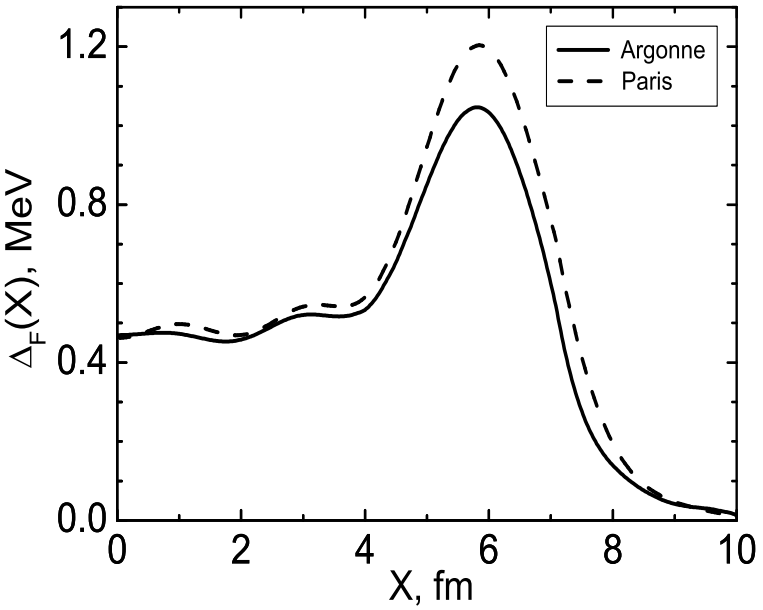

Figure 4: The Fermi averaged gap $\Delta_{\rm F}(X)$ for the Argonne v_{18} potential (solid line) and the Paris potential (dashes).

that the parameters of the EPI determining Δ change in the vicinity of the drip line has been ignored so far. It is hardly possible to address this issue

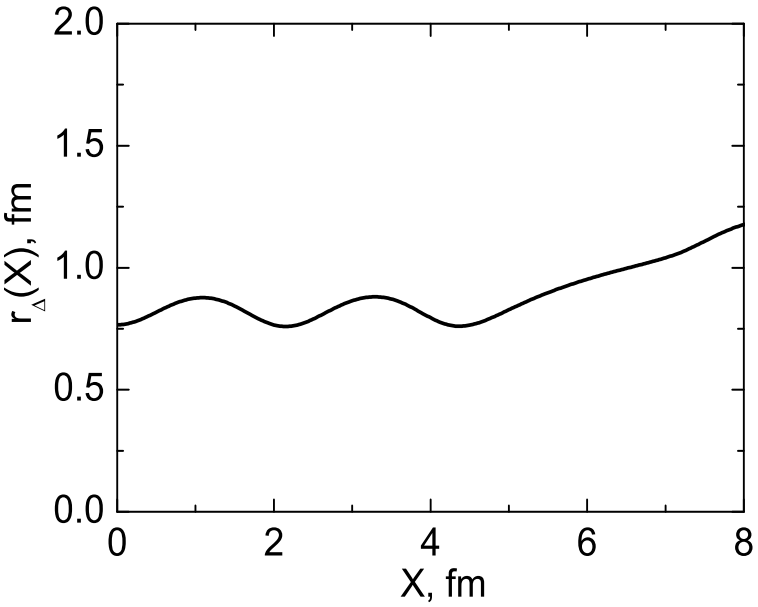

Figure 5: The rms radius of the gap $\Delta_{\rm F}(X)$ for the Argonne v_{18} potential.

within a phenomenological approach. This requires the use of the *ab initio* methods which start from a free NN-interaction.

Such a study was carried out in [17] for the Paris potential. Dependence of Δ on μ turned out to be model dependent provided the mean field $U(x)$ is not found self-consistently. The matter is that, as it was shown in [18, 19], the potential well $U(x)$ could change in vicinity of the drip point significantly due to dependence of the scalar Landau–Migdal amplitudes [11] on μ. As far as this problem is not solved up to now, two models were examined in [17]. In the first one (Model 1), the depth of the potential well U_0=−50 MeV is fixed, the central density increasing with decrease of $|\mu|$. In the second model (Model 2), the central density is considered to be a constant, the value of $|U_0|$ decreasing with decrease of $|\mu|$. It turned out that, with decrease of $|\mu|$, the gap value decreases in the first model and increases in the second one. In addition, the μ dependence of the so-called gap-shape function was examined in [17]. This quantity is defined as the ratio

$$\chi_{\rm F}(X) = \frac{\Delta_{\rm F}(X)}{\Delta_{\rm F}(0)}. \tag{29}$$

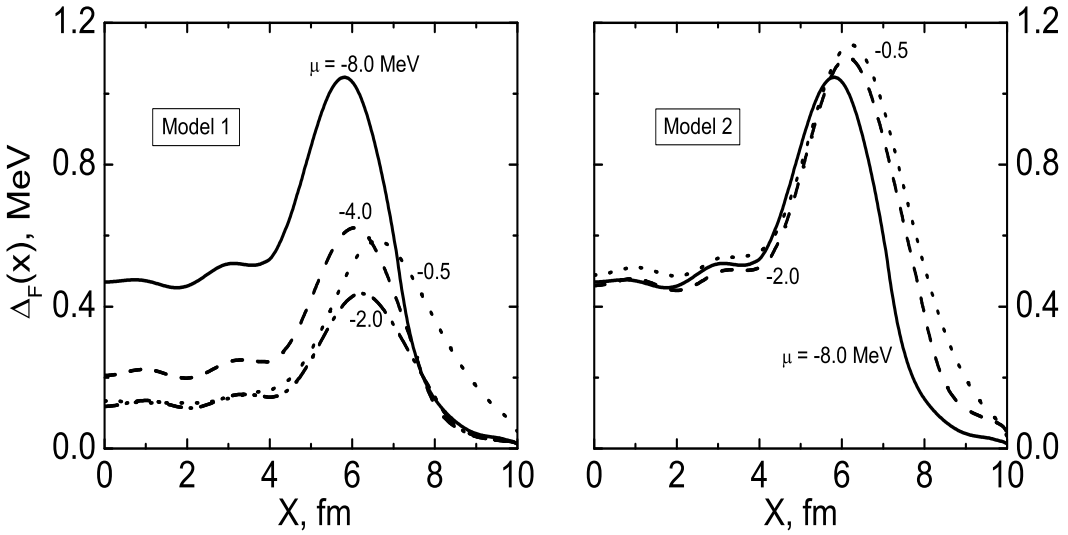

Figure 6: The Fermi averaged gap $\Delta_{\rm F}(X)$ for different values of the chemical potential μ.

It determines directly the effect of the surface enhancement of the gap [20, 21]. It turned out that this effect grows with decrease of $|\mu|$ within both the models.

Now we carry out analogous calculations for the Argonne force v_{18}. Dependence of the gap on the chemical potential for both the models is displayed in Fig. 6. In general, it repeats the behavior of the gap in the case of the Paris potential [17]. The main origin of the effect is the μ-dependence of the EPI which is shown in Fig. 7. In the first model, with decrease of $|\mu|$, the EPI becomes a little stronger in the asymptotic region and weaker inside the slab. The first effect originates from closeness to the pole in the free NN-scattering amplitude, the second one, due to growing of the local value of the Fermi momentum. It turned out that, with diminishing of $|\mu|$, the second reason dominates and Δ falls, and only at very small $|\mu|$ the surface enhancement of the EPI overcomes. In the second model, the EPI inside the slab doesn't practically depend on μ, and only the surface effect remains. Therefore in this case the gap value is growing with $|\mu|$ decreasing, but the effect is rather small.

In the first model, the μ-dependence effect is much more pronounced for the gap-shape function, see Fig. 8, left panel. In this case, the surface

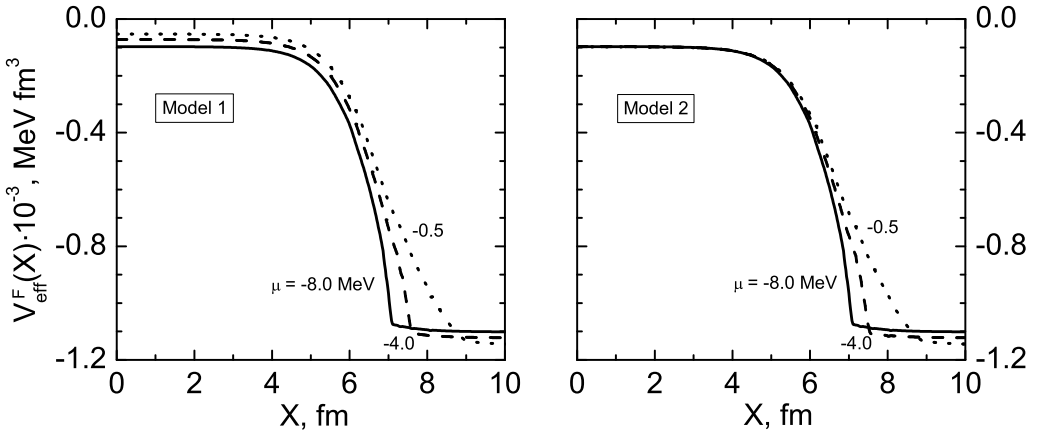

Figure 7: The Fermi averaged EPI $\mathcal{V}^{\rm F}_{\rm eff}(X)$ for different values of the chemical potential μ.

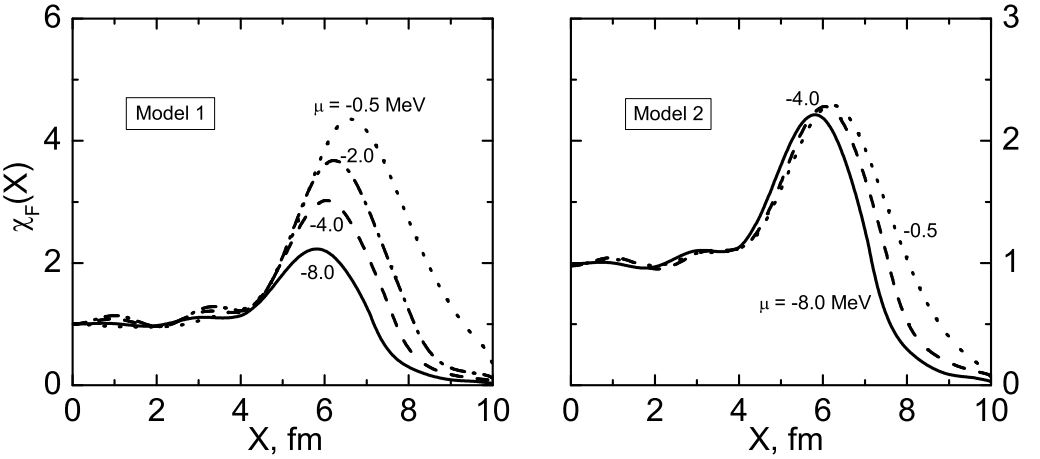

Figure 8: The gap shape function $\chi(X)$ for different values of the chemical potential μ.

enhancement of the gap becomes stronger with decrease of $|\mu|$, the effect being monotonic. It occurs because the nominator in (29) diminishes slower than the denominator. In the second model, the denominator in (29) almost doesn't depend on μ, and qualitatively the μ-dependence of gap-shape function repeats that of the gap itself.

5 Conclusions

We solved the microscopic gap equation for $^1S_0$ pairing in a nuclear slab for the Argonne v_{18} NN-potential. The slab is embedded into the Saxon-Woods potential well $U(x)$ with parameters typical for heavy nuclei. The width parameter $L = 6$ fm was chosen to mimic nuclei of the tin region examined in [2]. The features of the gap function obtained are very close to those found previously for the separable form of the Paris potential [3], but the absolute value of Δ turned out to be 10% less. This difference should be attributed to essentially different form of the free NN-potentials used which is the main input of the microscopic gap equation. Evidently, it may be considered as the upper estimate of the uncertainty originating from the specific choice of the NN-potential. Indeed, the two potentials are very contrast to each other, the Argonne force being rather soft and the Paris one, very hard. The diagonal matrix elements of Δ obtained are about 1.1 MeV which could be compared with the experimental value of $\Delta \simeq 1.3$ MeV in tin isotopes with $A \simeq 120$. On the other hand, the gap value obtained is significantly bigger than $\Delta \simeq 0.7$ MeV found in [2] where the lack of the gap was attributed to the contribution of the surface vibrations. Omitting the discussion of possible uncertainties in calculating these corrections (see, e.g., [10]), we mention only that the contribution of about 20% was obtained in [22] for the process under consideration. This estimate agrees with our calculations.

We think that different values of the effective nucleon mass m^* used is the main reason of the contradiction under discussion. In [2] the coordinate dependent effective mass $m^*(r)$ was used from the Sly4 force [6] which is essentially less than the bare nucleon mass, $m^* = m$, used by us. The latter is chosen in accordance with prescriptions of [7] and [8] which are based, in particular, on the analysis of the single-particle spectra of magic nuclei. Indeed, it is well known that the use of $m^* < m$ in any Skyrme-type forces results in the single-particle spectra which are significantly decompressed.

We analyzed also the dependence of the gap on the chemical potential μ. The result turned out to be model dependent in the approach with the potential well $U(x)$ considered as an input of the calculation scheme. In the first model, the depth U_0=−50 MeV is fixed, the central density increasing with decrease of $|\mu|$. In this case, the value of Δ decreases with diminishing of $|\mu|$ and only at very vicinity of the drip point it begins to grow. A different behavior was found of the gap-shape function which characterizes the surface enhancement of the gap. This quantity turned out to be mono-

tonically increasing with decrease of $|\mu|$. In the second model, the central density is supposed to be constant, the depth of $U(x)$ decreasing with decrease of $|\mu|$. In this case, the μ-dependence effect is less pronounced but the gap value and gap-shape function grow both with decrease of $|\mu|$. Thus, a self-consistent calculation of the potential well depending on μ is necessary to clarify the properties of nuclear pairing in the drip line vicinity. In this case, a μ-dependence of the effective force should be taken into account [18, 19] if one deals with the phenomenological approach.

6 Acknowlegements

The authors are highly thankful to S.T. Belyaev and S.V. Tolokonnikov for helpful discussions. This research was partially supported by the Grant NSh-8756.2006.2 of the Russian Ministry for Science and Education and by the RFBR grants 06-02-17171-a and 07-02-00553-a.

References

[1] F. Barranco, R. A. Broglia, H. Esbensen, and E. Vigezzi, Phys. Lett. B **390** (1997) 13.

[2] F. Barranco, R. A. Broglia, G. Colo, G. Gori, E. Vigezzi, and P. F. Bortignon. Eur. Phys. J. A 21 (2004) 57.

[3] S. S. Pankratov, M. Baldo, U. Lombardo, E. E. Saperstein, and M. V. Zverev, Nucl. Phys. A 765 (2006) 61.

[4] M. Lacombe, B. Loiseaux, J. M. Richard, R. Vinh Mau, J. Côté, D. Pirès and R. de Tourreil, Phys. Rev. C 21 (1980) 861.

[5] M. Baldo, J. Cugnon, A. Lejeune, U. Lombardo, Nucl. Phys. A 515 (1990) 409.

[6] E. Chabanat, P. Bonche, P. Haensel, J. Meyer, and R. Schaeffer, Nucl. Phys. A 627 (1997) 710.

[7] V. A. Khodel and E. E. Saperstein, Phys. Rep. 92 (1982) 183.

[8] S. A. Fayans, S. V. Tolokonnikov, E. L. Trykov, and D. Zawischa, Nucl. Phys. A 676 (2000) 49.

[9] R. B. Wiringa, V. G. J. Stoks, and R. Schiavilla, Phys. Rev. C 51 (1995) 38.

[10] M. Baldo, U. Lombardo, E. E. Saperstein, M. V. Zverev, Phys. Rep. 391 261 (2004).

[11] A. B. Migdal, Theory of finite Fermi systems and applications to atomic nuclei (Wiley, New York, 1967).

[12] P. Ring, P. Schuck, The nuclear many-body problem (Springer, Berlin, 1980).

[13] J. Haidenbauer, W. Plessas, Phys. Rev. C 30 (1984) 1822.

[14] J. Haidenbauer, W. Plessas, Phys. Rev. C 32 (1985) 1424.

[15] J. Dobaczewski, H. Flocard, and J. Treiner, Nucl. Phys. A 422 (1984) 103.

[16] J. Dobaczewski *et al.*, Phys. Rev. C 53 (1996) 2809.

[17] S. S. Pankratov, E. E. Saperstein, and M. V. Zverev, Phys. At. Nucl. 69 (2006) 2009.

[18] M. Baldo, U. Lombardo, E. E. Saperstein, M. V. Zverev, Phys. Lett. B 533 (2002) 17.

[19] E. E. Saperstein, S. V. Tollokonnikov, JETP Lett, 78 (2003) 795.

[20] M. Baldo, U. Lombardo, E. E. Saperstein, M. V. Zverev, Phys. Lett. B 459 (1999) 437.

[21] M. Baldo, M. Farine, U. Lombardo, E. E. Saperstein, P. Schuck and M. V. Zverev, Eur. Phys. J. A 18 (2003) 17.

[22] A. V. Avdeenkov, S. P. Kamerdzhiev, JETP Lett. 69 (1999) 715.